Article

2'-Mercaptonucleotide Interference Reveals Regions of Close Packing within Folded RNA Molecules

Jason P. Schwans, Cecilia N. Cortez, Joe M. Olvera, and Joseph A. Piccirilli

J. Am. Chem. Soc., **2003**, 125 (33), 10012-10018• DOI: 10.1021/ja035175y • Publication Date (Web): 29 July 2003

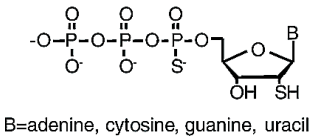

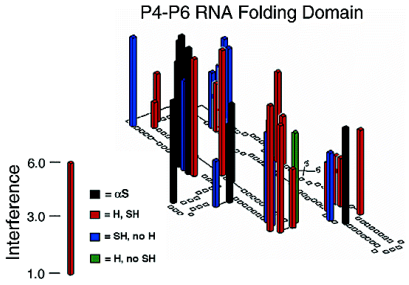

More About This Article

Additional resources and features associated with this article are available within the HTML version:

- Supporting Information
- Links to the 7 articles that cite this article, as of the time of this article download
- Access to high resolution figures
- Links to articles and content related to this article
- Copyright permission to reproduce figures and/or text from this article

View the Full Text HTML

J|A|C|S
ARTICLES
Published on Web 07/29/2003

2′-Mercaptonucleotide Interference Reveals Regions of Close Packing within Folded RNA Molecules

Jason P. Schwans, Cecilia N. Cortez, Joe M. Olvera, and Joseph A. Piccirilli*

Contribution from the Howard Hughes Medical Institute, Departments of Biochemistry and Molecular Biology, and Chemistry, The University of Chicago, Chicago, Illinois 60637

Received March 15, 2003; E-mail: jpicciri@midway.uchicago.edu

Abstract: The 2′-hydroxyl group makes essential contributions to RNA structure and function. As an approach to assess the ability of a mercapto group to serve as a functional analogue for the 2′-hydroxyl group, we synthesized 2′-mercaptonucleotides for use in nucleotide analogue interference mapping. To correlate the observed interference effects with tertiary structure, we used the independently folding ΔC209 P4-P6 domain from the *Tetrahymena* group I intron. We generated populations of ΔC209 P4-P6 molecules containing 2′-mercaptonucleotides located randomly throughout the domain and separated the folded molecules from the unfolded molecules by nondenaturing gel electrophoresis. Iodine-induced cleavage of the RNA molecules revealed the sites at which 2′-mercaptonucleotides interfere with folding. These interferences cluster in the most densely packed regions of the tertiary structure, occurring only at sites that lack the space and flexibility to accommodate a sulfur atom. Interference mapping with 2′-mercaptonucleotides therefore provides a method by which to identify structurally rigid and densely packed regions within folded RNA molecules.

Introduction

Sulfur substitution endows nucleic acids with unique physiochemical properties that empower biological chemists to elucidate fundamental features of nucleic acid structure and function. Virtually every oxygen atom on the nucleobases, sugar, and phosphoryl group has succumbed to sulfur modification.[1−3] Nevertheless, substitution of the 2′-hydroxyl group in RNA by a mercapto (SH) group has received relatively little attention, despite the potential of 2′-mercaptonucleosides as probes for the role of the 2′-hydroxyl group in RNA.[4] 2′-Mercaptonucleosides were first synthesized several decades ago, but most investigations of their properties have focused on the nucleoside or nucleotide level.[5] Although strategies for their incorporation into RNA oligonucleotides have become available recently,[6] the ability of the mercapto group to serve as a functional analogue for the 2′-hydroxyl group remains largely unexplored.[7] Just what features of RNA structure and function could 2′-mercaptonucleotides expose and how effectively can they mimic natural nucleotides in mediating tertiary interactions? To address these questions, we synthesized 2′-mercapto-α-thiotriphosphate analogues of adenosine, cytidine, guanosine, and uridine (Chart 1) for use in nucleotide analogue interference mapping.[8] To evaluate the structural and energetic basis of 2′-mercaptonucleotide interference, we used as a model system the structurally and biochemically well-defined P4-P6 independently folding RNA domain.[9] We obtained a "macromolecular profile"

(1) For examples of sulfur modification in the nucleobase, see the following and references therein: (a) Sontheimer, E. J. *Mol. Biol. Rep.* **1994**, *20*, 35. (b) Earnshaw, D. J.; Gait, M. J. *Biopolymers* **1998**, *48*, 39. (c) Yu, Y.-T. *Methods Enzymol.* **2000**, *318*, 71. (d) Favre, A.; Saintome, C.; Fourrey, J.-L.; Clivio, P.; Laugaa, P. *J. Photochem. Photobiol., B* **2000**, *42*, 109.

(2) For examples of sulfur modification in the sugar, see the following and references therein: (a) Bellon, L.; Morvan, F.; Barascut, J. L.; Imbach, J. L. *Biochem. Biophys. Res. Commun.* **1992**, *184*, 797. (b) Piccirilli, J. A.; Vyle, J. S.; Caruthers, M. H.; Cech, T. R. *Nature* **1993**, *361*, 85. (c) Zhou, D.-M.; Usman, N.; Wincott, F. E.; Matulic-Adamic, J.; Orita, M.; Zhang, L.-H.; Komiyama, M.; Kumar, P. K. R.; Taira, K. *J. Am. Chem. Soc.* **1996**, *118*, 5862. (d) Kuimelis, R. G.; McLaughlin, L. W. *Biochemistry* **1996**, *35*, 5308. (e) Hancox, E. L.; Walker, R. T. *Nucloside Nucleotides* **1996**, *15*, 135. (f) Weinstein, L. B.; Earnshaw, D. J.; Cosstick, R.; Cech, T. R. *J. Am. Chem. Soc.* **1996**, *118*, 10341. (g) Thomson, J. B.; Patel, B. K.; Jimenez, V.; Eckart, K.; Eckstein, F. *J. Org. Chem.* **1996**, *61*, 6273.

(3) For examples of phosphorothioate modifications, see the following and references therein: (a) Eckstein, F. *Angew. Chem.* **1983**, *95*, 431. (b) Eckstein, F. *Annu. Rev. Biochem.* **1985**, *54*, 367. (c) Ruffner, D. E.; Uhlenbeck, O. C. *Nucleic Acids Res.* **1990**, *18*, 6025. (d) Verma, S.; Eckstein, F. *Annu. Rev. Biochem.* **1998**, *67*, 99. (e) Shan, S.; Kravchuk, A. V.; Piccirilli, J. A.; Herschlag, D. *Biochemistry* **2001**, *40*, 5161. (f) Eckstein, F. *Biochimie* **2002**, *84*, 841. (g) Huppler, A.; Nikstad, L. J.; Allmann, A. M.; Brow, D. A.; Butcher, S. E. *Nat. Struct. Biol.* **2002**, *9*, 431.

(4) For examples of the role of the 2′-hydroxyl group in RNA structure and function, see the following and references therein: (a) Saenger, W. *Principles of Nucleic Acid Structure. Springer Advanced Text in Chemistry*; Springer-Verlag: New York, 1984. (b) Pyle, A. M.; Cech, T. R. *Nature* **1991**, *350*, 628. (c) Abramovitz, D. L.; Friedman, R. A.; Pyle, A. M. *Science* **1996**, *271*, 1410. (d) Egli, M.; Portmann, S.; Usman, N. *Biochemistry* **1996**, *35*, 8489. (e) Strobel, S. A.; Doudna, J. A. *Trends Biochem. Sci.* **1997**, *22*, 26. (f) Sjogren, A.-S.; Pettersson, E.; Sjoberg, B.-M.; Stromberg, R. *Nucleic Acids Res.* **1997**, *25*, 648. (g) Batey, R. T.; Rambo, R. P.; Doudna, J. A. *Angew. Chem.* **1999**, *38*, 2327. (h) Shan, S.; Yoshida, A.; Sun, S.; Piccirilli, J. A.; Herschlag, D. *Proc. Natl. Acad. Sci. U.S.A.* **1999**, *96*, 12299. (i) Gordon, P. M.; Sontheimer, E. J.; Piccirilli, J. A. *Biochemistry* **2000**, *39*, 12939. (j) Doherty, E. A.; Batey, R. T.; Masquida, B.; Doudna, J. A. *Nat. Struct. Biol.* **2001**, *8*, 339.

(5) (a) Ryan, K. J.; Acton, E. M.; Goodman, L. *J. Org. Chem.* **1971**, *36*, 2646. (b) Imazawa, M.; Ueda, T.; Ukita, T. *Chem. Pharm. Bull.* **1975**, *23*, 604. (c) Patel, A. D.; Schrier, W. H.; Nagyvary, J. *J. Org. Chem.* **1980**, *45*, 4830. (d) Divakar, K. J.; Mottoh, A.; Reese, C. B.; Sanghvi; Y. S. *J. Chem. Soc., Perkin Trans. I* **1990**, 969. (e) Marriott, J. H.; Mottahedeh, M.; Reese, C. B. *Carbohydr. Res.* **1991**, *216*, 257. (f) Dantzman, C. L.; Kiessling, L. L. *J. Am. Chem. Soc.* **1996**, *118*, 11715.

(6) (a) Hamm, M. L.; Piccirilli, J. A. *J. Org. Chem.* **1997**, *62*, 3415. (b) Raines, K. R.; Gottlieb, P. A. *RNA* **1998**, *4*, 340.

(7) (a) Earnshaw D. J.; Hamm, M. L.; Piccirilli, J. A.; Karpeisky, A.; Biegelman, L.; Ross, B. S.; Monoharan, M.; Gait, M. J. *Biochemistry* **2000**, *39*, 6410. (b) Hamm, M. L.; Schwans, J. P.; Piccirilli, J. A. *J. Am. Chem. Soc.* **2000**, *122*, 4223. (c) Hamm, M. L.; Nikolic, D.; van Breemen, R. B.; Piccirilli, J. A. *J. Am. Chem. Soc.* **2000**, *122*, 12069.

 10.1021/ja035175y CCC: $25.00

Chart 1. 2′-Mercaptonucleoside-α-thiotriphosphates

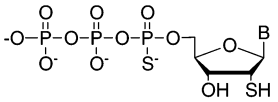

B = adenine, cytosine, guanine, uracil

showing that 2′-mercaptonucleotides reveal regions of close packing and structural rigidity within folded RNA molecules.

Results and Discussion

Raines and Gottlieb synthesized 2′-mercaptocytidine triphosphate using $POCl_3$ phosphorylation of 2′-deoxy-2′-(2-nitrophenyldithio)cytidine followed by reaction with pyrophosphate and subsequent reduction of the disulfide.[6b] We could not generate the corresponding α-thiotriphosphates using analogous reaction conditions with $PSCl_3$, however. Instead, we prepared the α-thiotriphosphates from the more stable 2′-*tert*-butyldisulfenyl[10] nucleosides using a one-pot/two-step reaction sequence with pyridine as both solvent and activating agent.[11] Subsequent reduction of the disulfide with DTT provided the desired 2′-mercaptonucleoside α-thiotriphosphates. We chose the ΔC209 P4-P6 domain[12] from the *Tetrahymena* ribozyme as the system with which to challenge 2′-mercaptonucleotides.[9] P4-P6 represents one of the largest RNAs to date whose folding has been characterized thermodynamically,[13] kinetically,[14] and crystallographically.[9b,c,h] We incorporated the analogues randomly throughout the ΔC209 P4-P6 domain by in vitro transcription using the mutant Y639F T7 RNA polymerase.[6b,15] I_2 sequencing[16] of the population revealed that the polymerase incorporated the analogues evenly throughout the RNA transcript at a level of approximately 1−5 substitutions per molecule (data not shown).[9b,g] We established that the 2′-SH groups remain intact following polyacrylamide gel electrophoresis (PAGE) purification and isolation of the RNA.[17,18]

The P4-P6 domain undergoes a tertiary folding transition in a Mg^{2+}-dependent manner (eq 1).[9] The folding transition renders the domain more compact such that folded molecules ($F{\cdot}nMg^{2+}$) migrate faster than unfolded molecules (U) during nondenaturing PAGE.[9,13]

$$U + nMg^{2+} \rightleftharpoons F{\cdot}nMg^{2+} \qquad (1)$$

The Mg^{2+} concentration dependence of the electrophoretic mobility of the domain relative to a permanently unfolded control molecule[9a] quantitatively describes the folding transition. The apparent standard free-energy change associated with the midpoint of the tertiary folding transition is given by $\Delta G^{\circ\prime} = n\mathrm{RT}\ \ln[Mg^{2+}]_{1/2}$,[13] where n represents the experimentally determined Hill coefficient and $[Mg^{2+}]_{1/2}$ gives the folding midpoint, the magnesium concentration at which the P4-P6 molecules equally populate the folded and unfolded states. For ΔC209 P4-P6, n equals 4 and $[Mg^{2+}]_{1/2}$ equals 0.45 mM $MgCl_2$.[9h]

We allowed the population of ΔC209 P4-P6 to fold[19] and electrophoresed them through a nondenaturing polyacrylamide gel.[9d,f] We excised those species with the same mobility as folded native ΔC209 P4-P6. Exposure of these selected RNA molecules to I_2 induces cleavage at all of the phosphorothioate linkages, revealing the location of 2′-mercaptonucleotides within the RNA.[16] Gaps in the resulting cleavage ladder as compared to the phosphorothioate control reveal sites at which 2′-mercaptonucleotides interfere with the tertiary folding transition (Figure 1).[8,9d,f] To achieve maximal sensitivity to folding interference without compromising signal, we conducted the gel selection experiments at $[Mg^{2+}]_{1/2}$ (0.45 mM $MgCl_2$). Under these conditions, the gel mobility shift assay detects energetic effects as small as 0.2 kcal/mol.[20]

2′-Mercaptonucleotide interference occurs at 24 of the 140 possible sites in the ΔC209 P4-P6 domain (Figure 2, red and blue bars). Little interference occurs in simple duplex regions, suggesting that the minor groove of A-form helical RNA readily accommodates the bulky mercapto group. Instead, the interferences occur primarily in the single-stranded regions of ΔC209 P4-P6, spanning the entire secondary structure of the domain. Elevated Mg^{2+} concentration (2.0 mM Mg^{2+}, Figure 2B) attenuates most of the interferences, underscoring the need to conduct these experiments near the midpoint of the folding transition. This Mg^{2+}-induced signal attenuation reveals an upper limit for the energetic destabilization imposed by the mercapto group ($\Delta\Delta G^{\circ\prime} = -n\mathrm{RT}\ \ln([0.45\ \mathrm{mM}\ Mg^{2+}]/[2.0\ \mathrm{mM}\ Mg^{2+}] = 3.5$ kcal/mol).[21]

To explore the physical basis of 2′-mercaptonucleotide interference, we obtained for comparison a 2′-deoxynucleotide (2′-H) interference map, which allows us to classify each residue in ΔC209 P4-P6 according to its 2′-SH/2′-H interference profile. Deoxynucleotide interference functionally distinguishes residues bearing dispensable 2′-hydroxyl groups from those bearing 2′-

(8) (a) Waring, R. B. *Nucleic Acids Res.* **1989**, *17*, 10281. (b) Christian, E. L.; Yarus, M. *J. Mol. Biol.* **1992**, *228*, 743. (c) Strobel, S. A.; Shetty, K. *Proc. Natl. Acad. Sci. U.S.A.* **1997**, *94*, 2903. (d) Ortoleva-Donnelly, L.; Szewczak, A. A.; Gutell, R. R.; Strobel, S. A. *RNA* **1998**, *4*, 498. (e) Strobel, S. A. *Curr. Opin. Struct. Biol.* **1999**, *9*, 346. (f) Ryder, S. P.; Strobel, S. A. *Methods* **1999**, *1*, 38. (g) Ryder, S. P.; Ortoleva-Donnelly, L.; Kosek, A. B.; Strobel, S. A. *Methods Enzymol.* **2000**, *317*, 92 and references therein.

(9) (a) Murphy, F. L.; Cech, T. R. *Biochemistry* **1993**, *32*, 5291. (b) Cate, J. H.; Gooding, A. R.; Podell, E.; Zhou, K.; Golden, B. L.; Kundrot, C. E.; Cech, T. R.; Doudna, J. A. *Science* **1996**, *273*, 1687. (c) Cate, J. H.; Doudna, J. A. *Structure* **1996**, *4*, 1221. (d) Cate, J. H.; Hanna, R. L.; Doudna, J. A. *Nat. Struct. Biol.* **1997**, *4*, 553. (e) Szewczak, A. A.; Cech, T. R. *RNA* **1997**, *3*, 838. (f) Basu, S.; Strobel, S. A. *RNA* **1999**, *5*, 1399. (g) Juneau, K.; Cech, T. R. *RNA* **1999**, *5*, 1119. (h) Juneau, K.; Podell, E.; Harrington, D. J.; Cech, T. *Structure* **2001**, *9*, 221.

(10) Pastuszak, J. J.; Chimiak, A. *J. Org. Chem.* **1981**, *46*, 1868.

(11) Fisher, B.; Chulkin, A.; Boyer, J. L.; Harden, K. T.; Gendron, F.-P.; Beaudoin, A. R.; Chapal, J.; Hillaire-Buys, D.; Petit, P. *J. Med. Chem.* **1999**, *42*, 3636.

(12) ΔC209 has the same sequence and global fold as the natural P4-P6 domain but lacks cytidine 209.[9g,h]

(13) (a) Silverman, S. K.; Cech, T. R. *Biochemistry* **1999**, *38*, 8691. (b) Silverman, S. K.; Cech, T. R. *RNA* **2001**, *7*, 161.

(14) Silverman, S. K.; Deras, M. L.; Woodson, S. A.; Scaringe, S. A.; Cech, T. R. *Biochemistry* **2000**, *39*, 12465.

(15) Sousa, R.; Padilla, R. *EMBO J.* **1995**, *14*, 4609.

(16) Gish, G.; Eckstein, F. *Science* **1988**, *240*, 1520.

(17) Bonaventura, C.; Bonaventura, J.; Stevens, R.; Millington, D. *Anal. Biochem.* **1994**, *222*, 44.

(18) The following data establish the integrity of the mercapto group: (1) Following purification by DTT PAGE (see Experimental Section), a synthetic oligonucleotide containing a single 2′-mercaptocytidine residue reacted quantitatively with Thiolyte MQ, (2) transcription of ^{ppp}GAUGGC in the presence of 2′-mercaptouridine triphosphate and no UTP generates a transcript that reacts quantitatively with Thiolyte MQ, and (3) incubation with biotin-PEG_3-maleimide followed by streptavidin shifted the electrophoretic mobility of the entire population of ΔC209 molecules (data not shown).

(19) Folding conditions: 50 °C for 10 min followed by slow cooling to room temperature; Tris-Borate pH 8.3; 5% glycerol; $MgCl_2$ as indicated. Under these conditions, the gel mobility shift assay gives the same n value and $[Mg^{2+}]_{1/2}$ as reported by Juneau et al.[9h]

(20) Site-specific substitution of A183 with 2′-deoxyadenosine destabilized P4-P6 tertiary folding by 0.2 kcal/mol.[13] The gel mobility shift assay detects 2′-deoxyadenosine interference at position 183.

(21) We assume here that the individual mercaptan-modified RNA molecules undergo a Mg^{2+}-dependent, two-state folding transition with the same n value as the unmodified ΔC209 P4-P6.

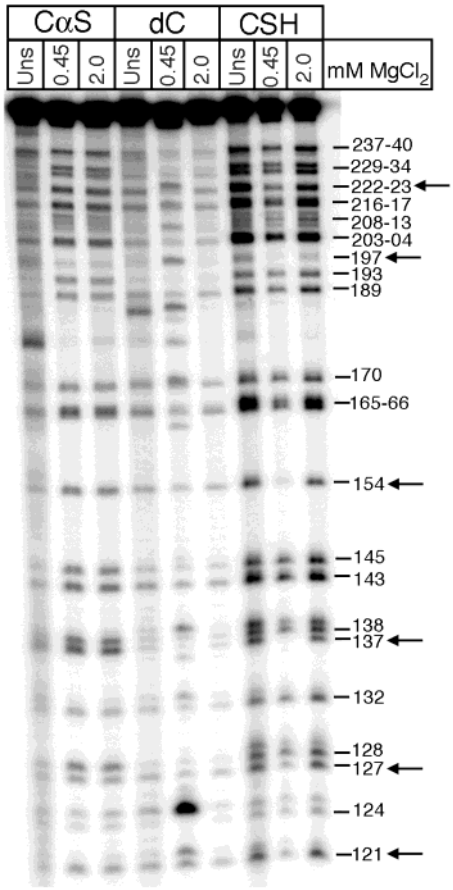

Figure 1. RNA folding interferences induced by nucleotide analogues. Shown are representative sequencing ladders of ΔC209 P4-P6 populations containing phosphorothioates at cytidine (CαS), 2′-deoxycytidine (dC), or 2′-mercaptocytidine (CSH) residues. Gaps in the I_2-induced cleavage pattern of the folded population reveal the sites of interference. The unselected lane (Uns) gives the extent and location of analogue incorporation during transcription and indicates an even distribution of the analogue throughout the RNA. Arrows indicate sites of interference: 121, 127, 137, 154, 197, 222-23. Shorter electorophoresis times retain the smaller RNA fragments and reveal interference at C109 (data not shown). As a control for degradation, we also analyzed samples without I_2 incubation (data not shown).

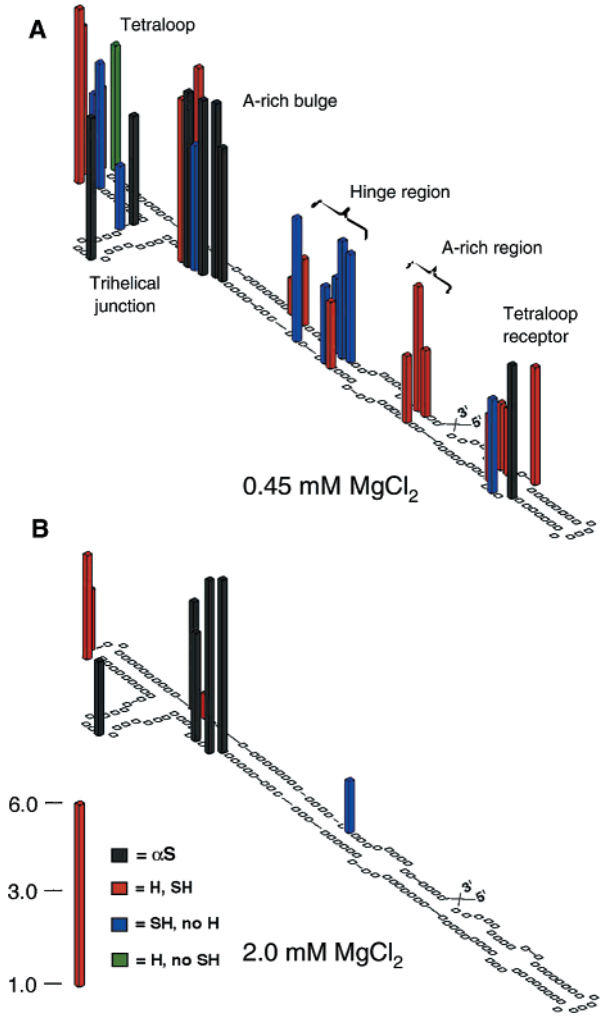

Figure 2. ΔC209 P4-P6 secondary structure with histogram indicating the sites of 2′-H and 2′-SH interference at (A) 0.45 mM and (B) 2.0 mM $MgCl_2$. Red bars represent sites that exhibit interference with both analogues. Blue bars represent sites that exhibit 2′-SH interference uniquely. The green bar represents a site that exhibits 2′-H interference uniquely. Gray bars represent sites that exhibit phosphorothioate interference, which masks possible interference from the 2′-modification. Interference values were calculated as described by Ryder et al.[8g]

hydroxyl groups that provide a significant energetic contribution to folding (Figure 2, red and green bars). All deoxynucleotide interferences in P4-P6 occur at residues whose 2′-hydroxyl groups engage in hydrogen bonds, as was inferred from the crystal structure.[9b,h] Among these sites, only one exhibits no 2′-SH interference (Figure 2A, green bar): tetraloop residue G150, whose 2′-OH donates a hydrogen bond to N7 of A152. The absence of 2′-SH interference here indicates that a mercapto group at this site functionally mimics the hydrogen bonding interaction of the 2′-hydroxyl group. Although mercaptans form considerably weaker hydrogen bonds than do hydroxyl groups,[22] this interaction could provide a favorable thermodynamic contribution to folding as mercaptans undergo desolvation with considerably smaller energetic penalty than do hydroxyl groups.[23,24] The remaining sites of 2′-deoxynucleotide interference (Figure 2, red bars) exhibit 2′-SH interference, indicating that generally the 2′-mercapto group lacks the ability to supplant these important 2′-hydroxyl groups. Apparently, the spatial and geometric constraints imposed by the P4-P6 structure preclude effective hydrogen bonding with the mercapto group. 2′-SH interference at sites bearing dispensable 2′-hydroxyl groups (Figure 2, blue bars) must arise as a consequence of the sulfur atom rather than from disruption of a hydrogen bond. Interestingly, these sites flank the 2′-H/2′-SH interferences (Figure 2 and see below), suggesting that the sulfur may interfere by disrupting nearby tertiary interactions. When modeled into the ΔC209 P4-P6 structure, the sulfur atoms at all sites of 2′-SH interference penetrate the van der Waals volumes of nearby atoms (Figure 3). Presumably, the folded structure cannot accommodate the large sulfur atom without energetic penalty from short-range repulsions. Conversely, no such van der Waals overlap occurs at the sites that exhibit no 2′-SH interference.

To provide a global view of the 2′-hydroxyl groups within P4-P6, we modeled a sulfur atom at every residue in the space-filling representation of the molecule (Figure 4A).[9b,h] Most of

(22) Crampton, M. R. In *Chemistry of the −SH Group*; Pati, S., Ed.; Wiley-Interscience: New York, 1974; p 379.
(23) Fersht, A. *Trends Biochem. Sci.* **1987**, *12*, 301 and references therein.
(24) The thermodynamic contribution of these hydrogen bonds to the folded state of the RNA reflects an energy balance between the intrinsic strength of each hydrogen bond and the desolvation energy of the interacting partners. 2′-SH interference therefore reflects an unfavorable hydrogen bond exchange reaction between the hydrogen bonding partners and water in going from the unfolded to the folded state.

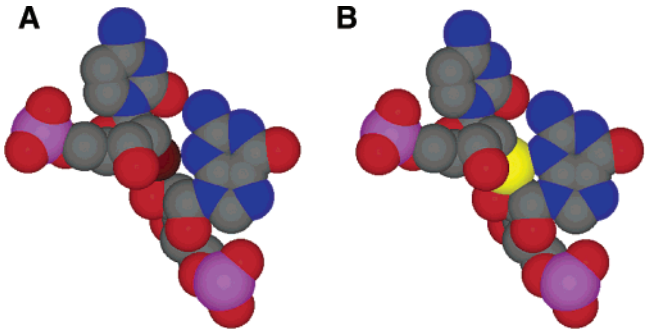

Figure 3. A structural basis for 2′-mercaptonucleotide interference. (A) Space-filling representation of residues C197 and G200 located in the hinge region. C197 bears a dispensable 2′-hydroxyl group (dark red sphere) that packs closely against the nucleobase G200. (B) A 2′-mercapto group at C197 penetrates the van der Waals volume of nearby atoms.

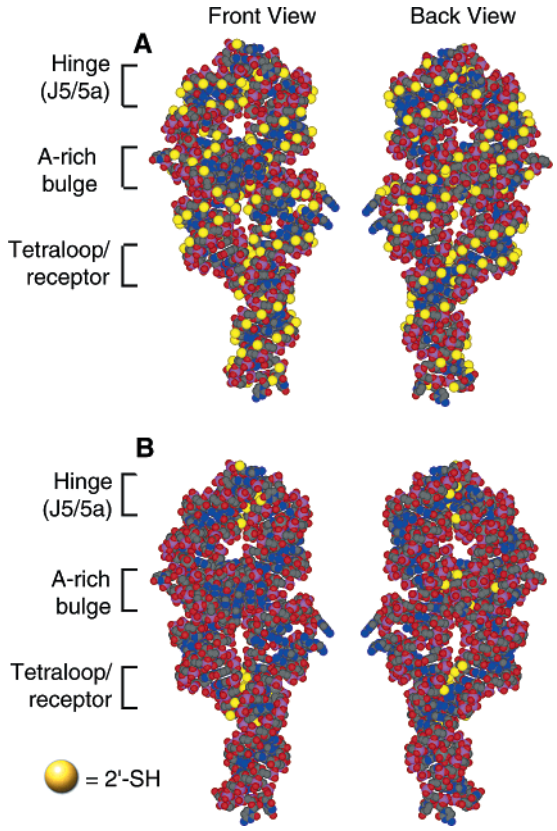

Figure 4. The spatial distribution of 2′-SH interferences in ΔC209 P4-P6. (A) Space-filling representation of the ΔC209 P4-P6 structure with all 2′-OH groups replaced by 2′-SH groups so as to highlight their locations in the molecule. Most 2′-OH groups line the rim of the minor groove on the solvent accessible surface. (B) Sites of 2′-mercaptonucleotide interference at 0.45 mM $MgCl_2$. Interferences cluster between the parallel stacked helices in the densely packed regions involved in tertiary contacts. Atomic coordinates are from PDB accession 1HR2.[9h]

the 2′-hydroxyl groups reside in the minor groove and other solvent accessible regions. Figure 4B highlights the locations at which 2′-mercaptonucleotides interfere with P4-P6 folding. Strikingly, most regions of the structure experience no 2′-SH interference. Instead, the interferences tightly cluster in the three most densely packed regions of the molecule: the tetraloop/receptor, the A-rich bulge/trihelical junction, and the hinge region (J5/5a). The residues in these regions experience significant surface area burial, engage in hydrogen bonding interactions via their 2′-hydroxyl groups, and exhibit strong deviations from A-form helical geometry.[9b,h]

Conclusions

We have used the plethora of microenvironments offered by a macromolecule of known structure to explore an atomic modification. Steric interactions dominate the response of RNA to 2′-mercaptonucleotide substitution, whereby the mercapto group acts as a 35 $Å^3$ sphere (a hydroxyl group occupies 13 $Å^3$)[25] that disrupts folding when the local environment lacks the flexibility and space to accommodate it. Consequently, 2′-mercaptonucleotides provide a method by which to expose structurally rigid and densely packed regions of folded RNA molecules.

Experimental Section

All reagents and anhydrous solvents were purchased from Aldrich; other solvents were from Fisher. All reactions using air-sensitive or moisture-sensitive reagents were carried out under an argon atmosphere. ^1H and ^{31}P NMR spectra were recorded on Bruker 500 or 400 MHz NMR spectrometers. ^1H chemical shifts are reported in ppm relative to tetramethylsilane. ^{31}P chemical shifts are reported relative to an external standard of 85% aqueous H_3PO_4. Mass spectra were obtained from the Department of Chemistry, University of California at Riverside, using a VG-ZAB instrument or from the Department of Chemistry, University of Chicago, using a HP ESI instrument. Merck silica gel (9385 grade, 230-400 mesh, 60 Å, Aldrich) was used for column chromatography. Silica gel on glass with fluorescent indicator (Aldrich) was used for TLC.

Nucleotide modifying enzymes were from Amersham Pharmacia or New England Biolabs. [γ-^{32}P]-Adenosine triphosphate was obtained from Perkin-Elmer Life Sciences. Nucleoside triphosphates were from Amersham Pharmacia, and 2′-ribo- and deoxy-α-triphosphates were from Glen Research. Biotin-PEG_3-maleimide was purchased from Pierce, and streptavidin was from Sigma. Denaturing polyacrylamide gel electrophoresis (DPAGE) was carried out using 6−9% polyacrylamide (Fisher; acrylamide:bis-acrylamide, 29:1) with 7 M urea and TBE (89 mM Tris, 89 mM boric acid; 2 mM EDTA). DTT gels (10 mM DTT/7 M urea/TBE) were cast and allowed to polymerize overnight. Gel loading buffer contained 8 M urea (J. T. Baker), 50 mM EDTA (pH 8.0, Fisher), 0.02% bromophenol blue (EM Science), 0.02% xylene cyanol FF (Kodak), and 10 mM DTT.

3′,5′-*O*-(Tetraisopropyldisiloxane-1,3-diyl)-2′-deoxy-2′-(*t*-butylthio)adenosine. 6-*N*-Benzoyl-9-[3,5-*O*-(1,1,3,3-tetraisopropyldisiloxane-1,3-diyl)-2-*O*-trifluoromethanesulfonyl-β-D-arabinofuranosyl]-adenine[5e] (838 mg, 1.13 mmol) was dissolved in DMSO. 2-Methyl-2-propanethiol (0.3 mL, 2.26 mmol, 2 equiv) was added followed by dropwise addition of 1,1,3,3-tetramethylguanidine (0.3 mL, 1.7 mmol, 1.5 equiv). After being stirred at room temperature for 2 h, the reaction was diluted with cold CH_2Cl_2 (20 mL). The solution was washed with saturated $NaHCO_3$ and dried over $MgSO_4$. Short column silica gel flash chromatography using 0−2% EtOH in CH_2Cl_2 gave the product. The material was dissolved in MeOH (25 mL) and cooled to 0 °C. NH_3 was bubbled into the solution until saturated. The solution was then allowed to warm to room temperature and stirred for 16 h. The solvent was evaporated, and the residue was purified by silica gel chromatography (0−2% EtOH in CH_2Cl_2) to give 3′,5′-*O*-(tetraisopropyldisiloxane-1,3-diyl)-2′-deoxy-2′-(*tert*-butylthio)adenosine (79% yield over the two steps) as a white foam.^1H NMR ($CDCl_3$, 400 MHz): δ 8.33 (s, 1H), 8.06 (s, 1H), 6.09 (d, 1H), 5.80 (bs, 2H), 4.87 (t, 1H), 4.09 (m, 5H), 1.25 (s, 9H), 1.05 (m, 28H). HRMS (FAB^+): calculated for $C_{26}H_{48}N_5O_4SSi_2$ (MH^+) 582.2979; found 582.2989.

2′-Deoxy-2′-(*t*-butylthio)adenosine. 3′,5′-*O*-(Tetraisopropyldisiloxane-1,3-diyl)-2′-deoxy-2′-(*tert*-butylthio)adenosine (131.5 mg, 0.226 mmol) was dissolved in THF (5 mL). TBAF·$3H_2O$ (71 mg, 0.271

(25) Ammon, H. *Struct. Chem.* **2001**, *12*, 205.

mmol) was added, and the solution turned slightly yellow. Within 15 min, TLC indicated the disappearance of the starting material. The solvent was evaporated, and the residue was dissolved in 5% MeOH/$CHCl_3$. Silica gel column chromatography (5−10% MeOH in $CHCl_3$) eluted the product as a white solid in 60% yield. ^{1}H NMR (CD_3OD, 500 MHz): δ 8.25 (s, 1H), 8.19 (s, 1H), 5.87 (d, 1H), 4.33 (d, 1H), 4.23 (bs, 1H), 4.09 (q, 1H), 3.95−3.76 (dd, 2H), 0.98 (s, 9H). HRMS (FAB$^+$): calculated for $C_{25}H_{22}N_5O_3S$ (MH^+) 340.1443; found 340.1445.

2′-Deoxy-2′-(2-nitrophenyldithio)adenosine. 2′-Deoxy-2′-(*tert*-butylthio)adenosine (259 mg, 0.763 mmol) was dissolved in glacial acetic acid (7 mL). 2-Nitrobenzenesulfenyl chloride (173 mg, 0.916 mmol, 1.2 equiv) was added, and the solution was stirred at room temperature for 16 h. The solution was concentrated, and the residue was purified by column chromatography (0−5% MeOH in $CHCl_3$) to give 2′-deoxy-2′-(2-nitrophenyldithio)adenosine (88% yield) as a yellow solid. ^{1}H NMR (CD_3OD, 500 MHz): δ 8.35 (s, 1H), 8.18 (s, 1H), 8.03 (t, 2H), 7.87 (s, 1H), 7.56 (t, 1H), 7.31 (t, 1H), 6.38 (d, 1H), 4.58 (d, 1H), 4.34 (m, 1H), 4.14 (m, 1H), 3.72 (m, 2H). MS (ESI): calculated for $C_{16}H_{17}N_6O_5S_2$ (MH^+) 437.06; found 437.0.

2′-Deoxy-2′-(*t*-butyldithio)adenosine. 2′-Deoxy-2′-(2-nitrophenyldithio)adenosine (47.5 mg, 0.109 mmol) was dissolved in 10% MeOH/$CHCl_3$ (5 mL). In a separate flask, 2-methyl-2-propanethiol (80 μL, 0.71 mmol), triethylamine (0.17 mL), and methanol (1.5 mL) were combined. The solution was transferred to the reaction flask and stirred for 3 h at room temperature. The reaction was concentrated, and the residue was purified by column chromatography (0−10% MeOH in $CHCl_3$) to give 2′-deoxy-2′-(*tert*-butyldithio)adenosine as a white solid in 89% yield. ^{1}H NMR (CD_3OD, 400 MHz): δ 8.29 (s, 1H), 8.14 (s, 1H), 6.15 (d, 1H), 4.55 (d, 1H), 4.26 (m, 1H), 4.17 (bs, 1H), 3.76−3.72 dd, 2H). MS (ESI): calculated for $C_{14}H_{22}N_5O_3S_2$ (MH^+) 372.12; found 372.0.

2′-Deoxy-2′-(*t*-butyldithio)cytidine. 2′-Deoxy-2′-(2-nitrophenyldithio)-cytidine[5d] (70 mg, 0.170 mmol) was dissolved in 10% MeOH/$CHCl_3$ (10 mL). In a separate flask, 2-methyl-2-propanethiol (115 μL, 1.02 mmol), triethylamine (277 μL), and methanol (2.8 mL) were combined. The solution was transferred to the reaction flask and stirred for 3 h at room temperature. The reaction was concentrated, and the residue was purified by column chromatography (0−10% MeOH in $CHCl_3$) to give the product as a white solid in 90% yield. ^{1}H NMR ($CDCl_3$, 400 MHz): δ 7.77 (d, 1H, J = 7.5 Hz), 6.06 (d, 1H, J = 9.0 Hz), 5.81 (d, 1H, J = 7.4 Hz), 4.30 (m, 1H), 3.89 (m, 1H), 3.61 (m, 3H), 1.14 (s, 9H). MS (ESI): calculated for $C_{13}H_{22}N_3O_4S_2$ (MH^+) 348.10; found 348.1.

2′-Deoxy-2′-(*t*-butyldithio)uridine. 2′-Deoxy-2′-(2-nitrophenyldithio)-uridine[5d] (94 mg, 0.243 mmol) was dissolved in 10% MeOH/$CHCl_3$ (12.5 mL). In a separate flask, 2-methyl-2-propanethiol (164 μL, 1.46 mmol), triethylamine (375 μL), and methanol (3.8 mL) were combined. The solution was transferred to the reaction flask and stirred for 3 h at room temperature. The reaction was concentrated, and the residue was purified by column chromatography (0−10% MeOH in $CHCl_3$) to give 2′-deoxy-2′-(*tert*-butyldithio)uridine as a white solid (90% yield). ^{1}H NMR ($CDCl_3$, 400 MHz): δ 7.96 (d, 1H, J = 8.1 Hz), 5.85 (d, 1H, J = 9.8 Hz), 5.77 (d, 1H, J = 8.1 Hz), 4.26 (d, 1H, J = 4.6 Hz), 4.03 (m, 1H), 3.78 (m, 2H), 3.63 (q, 1H), 1.35 (s, 9H). HRMS (FAB$^+$): calculated for $C_{13}H_{21}N_2O_5S_2$ (MH^+) 349.0879; found 349.0878.

9-[3,5-*O*-(1,1,3,3-Tetraisopropyldisiloxane-1,3-diyl)-2-*O*-trifluoromethanesulfonyl-*β*-D-arabinofuranosyl]guanosine. 9-[3,5-*O*-(1,1,3,3-Tetraisopropyldisiloxane-1,3-diyl)-2′-*β*-D-arabinofuranosyl]guanosine[26] (1.2 g, 2.28 mmol) and 4-(dimethylamino)pyridine (1.2 g, 13.2 mmol) were dissolved in CH_2Cl_2 (10 mL). The reaction mixture was cooled to 0 °C, and trifluoromethanesulfonyl chloride (0.46 g, 2.7 mmol) was added dropwise. The yellow solution was stirred for 10 min. The reaction mixture was partitioned between ice-cooled acetic acid/water (1:99, 25 mL) and extracted with CH_2Cl_2 (2 × 250 mL). The organic phase was combined and washed with ice-cold saturated aqueous $NaHCO_3$ and brine and was dried over $MgSO_4$. Column chromatography of the residue (0−5% MeOH in CH_2Cl_2) gave 9-[3,5-*O*-(1,1,3,3-tetraisopropyldisiloxane-1,3-diyl)-2-*O*-trifluoromethanesulfonyl-*β*-D-arabinofuranosyl]guanosine as a white solid in 51% yield. ^{1}H NMR ($CDCl_3$, 500 MHz): δ 7.69 (s, 1H), 6.19 (d, 2H), 5.34 (t, 1H), 4.85 (m, 1H), 4.04 (m, 2H), 3.85 (m, 1H), 1.07 (s, 9H), 0.99 (m, 28H).

3′,5′-*O*-(Tetraisopropyldisiloxane-1,3-diyl)-2′-deoxy-2′-(*t*-butylthio)guanosine. 9-[3, 5-*O*-(1,1,3,3-Tetraisopropyldisiloxane-1,3-diyl)-2-*O*-trifluoromethanesulfonyl-*β*-D-arabinofuranosyl]guanosine (500 mg, 0.76 mmol) was dissolved in DMSO (20 mL). 2-Methyl-2-propanethiol (137 mg, 1.52 mmol) and 1,1,3,3-tetramethylguanidine (175 mg, 1.52 mmol) were added, and the mixture was stirred for 24 h at room temperature. Saturated $NaHCO_3$ was added, and a precipitate formed. The precipitate was filtered, washed, and dried under vacuum. Column chromatography (0−5% EtOH in $CHCl_3$) gave 3′,5′-*O*-(tetraisopropyldisiloxane-1,3-diyl)-2′-deoxy-2′-(*tert*-butylthio)guanosine (360 mg, 79%) as a white solid. ^{1}H NMR ($CDCl_3$, 500 MHz): δ 8.08 (s, 1H), 5.88 (s, 1H), 4.65 (t, 1H), 3.85−4.17 (m, 4H), 1.18 (s, 9H), 0.98 (m, 28H). MS (ESI): calculated for $C_{26}H_{48}N_5O_5SSi_2$ (MH^+) 598.28; found 598.2.

3′,5′-*O*-(Tetraisopropyldisiloxane-1,3-diyl)-2′-(2-nitrophenyldithio)guanosine. 3′,5′-*O*-(Tetraisopropyldisiloxane-1,3-diyl)-2′-deoxy-2′-(*tert*-butylthio)guanosine (70 mg, 0.12 mmol) was dissolved in glacial acetic acid (5 mL). 2-Nitrobenzenesulfenyl chloride (68 mg, 0.36 mmol, 1.2 equiv) was added, and the reaction was stirred at room temperature for 24 h. The acetic acid was removed by evaporation. The resulting residue was purified by column chromatography (0−5% MeOH in $CHCl_3$) to give 2′-deoxy-2′-(2-nitrophenyldithio)guanosine (79 mg, 73%) as a yellow solid. ^{1}H NMR ($CDCl_3$, 500 MHz): δ 8.06 (m, 3H), 7.68 (bs, 2H), 7.52 (m, 2H), 7.25 (m, 2H), 5.97 (s, 1H), 4.78 (m, 1H), 3.76−4.10 (m, 4H), 1.01 (m, 28 H). MS (ESI): calculated for $C_{28}H_{43}N_6O_7S_2Si_2$ (MH^+) 695.21; found 695.1.

2′-Deoxy-2′-(2-nitrophenyldithio)guanosine. 9-[3,5-*O*-(1,1,3,3-Tetraisopropyldisiloxane-1,3-diyl)-2′-(2-nitrophenyldithio)-*β*-D-arabinofuranosyl]guanosine (180 mg, 0.26 mmol) was dissolved in THF (10 mL). TBAF (1 M in THF, 0.52 mL) was added; TLC indicated that the reaction was complete within 3 min. The solvent was evaporated, and the residue was purified by column chromatography (0−10% MeOH in $CHCl_3$) to give 2′-deoxy-2′-(2-nitrophenyldithio)guanosine (80 mg, 68%) as a yellow solid. ^{1}H NMR (CD_3OD, 400 MHz): δ 8.05 (d, 1H, J = 7.1 Hz), 7.94 (d, 1H, J = 8.1 Hz), 7.77 (s, 1H), 7.50 (t, 1H, J = 7.1 Hz), 7.27 (t, 1H, J = 7.1 Hz), 6.10 (d, 1H, J = 9.5 Hz), 4.51 (d, 1H, J = 5.2 Hz), 4.44 (m, 1H), 4.07 (m, 1H), 3.68 (m, 2H). MS (ESI): calculated for $C_{16}H_{15}N_6O_6S_2$ (MH^-) 452.05; found 451.0.

2′-Deoxy-2′-(*t*-butyldithio)guanosine. 2′-Deoxy-2′-(2-nitrophenyldithio)guanosine (60 mg, 0.130 mmol) was dissolved in 10% methanol/$CHCl_3$ (20 mL). In a separate flask, 2-methyl-2-propanethiol (24 μL, 0.26 mmol), triethylamine (70 μL), and methanol (3.0 mL) were combined. The solution was transferred to the reaction flask and stirred for 3 h at room temperature. The reaction was concentrated, and the resulting mixture was purified by column chromatography (0−10% MeOH in $CHCl_3$) to give 2′-deoxy-2′-(*tert*-butyldithio)guanosine (40 mg, 80% yield) as a white solid. ^{1}H NMR (CD_3OD, 400 MHz): δ 7.94 (s, 1H), 6.02 (d, 1H, J = 9.2 Hz), 4.50 (d, 1H, J = 5.1 Hz), 4.16 (m, 1H), 4.14 (s, 1H) 3.73−3.84 (dd, 2H), 1.15 (s, 9H). MS (ESI): calculated for $C_{14}H_{20}N_5O_4S_2$ (MH^-) 386.10; found 386.0.

General Method for the Synthesis of α-Thiotriphosphates. A suspension of the nucleoside (25 mg) and pyridine (3 mL) was heated with an air gun for several minutes until a clear solution was obtained. Following cooling of the solution to room temperature, proton sponge (20 mg, 2 equiv) was added. The solution was further cooled to 0 °C and stirred for 10 min. Thiophosphoryl chloride (10 μL, 2 equiv) was added dropwise, and the solution was stirred at 0 °C for 15 min. Tri-*n*-butylammonium pyrophosphate (500 mg), tri-*n*-butylamine (0.25 mL),

(26) Kawasaki, A. M.; Casper, M. D.; Freier, S. M.; Lesnik, E. A.; Zounes, M. C.; Cummins, L. L.; Gonzalez, C.; Cook, P. D. *J. Med. Chem.* **1993**, *36*, 831.

and DMF (2 mL) were combined in a separate flask and transferred under anhydrous conditions to the reaction flask via cannula. The reaction was stirred at 0 °C for 2 min. Triethylammonium bicarbonate (20 mL, 0.2 M) and proton sponge (20 mg) were then added, and the solution was stirred for 1 h at room temperature. The reaction mixture was purified by ion-exchange chromatography (Sephadex DEAE-A25) at room temperature using a gradient of triethylammonium bicarbonate (0.1−1.0 M). Fractions containing the α-thiotriphosphate were visualized by TLC, pooled, and dried. The material was purified further by reverse phase HPLC on a Beckman ODS Ultrasphere C_{18} reverse-phase column (10 × 250 mm) using a gradient of 0.1 M triethylammonium acetate (solvent A) and acetonitrile (solvent B). The following linear gradient program was used: 0−12% solvent B over 25 min to 40% solvent B over 40 min.

2′-Deoxy-2′-(*t*-butylthio)adenosine-α-thiotriphosphate. ^{31}P NMR (D_2O, 400 MHz): δ 44.2 m, −8.9 d, −22.8−23.1 m. HRMS (FAB): calculated for $C_{14}H_{23}N_5O_{11}P_3S_3^-$ (M^-) 625.9775; found 625.9770.

2′-Deoxy-2′-(*t*-butylthio)cytidine-α-thiotriphosphate. ^{31}P NMR (D_2O, 400 MHz): δ 41.1 m, −13 dd, −26.2 m. HRMS (FAB): calculated for $C_{13}H_{23}N_3O_{12}P_3S_3^-$ (M^-) 601.9662; found 601.9623.

2′-Deoxy-2′-(*t*-butylthio)guanosine-α-thiotriphosphate. ^{31}P NMR (D_2O, 500 MHz): δ 44 m, −10.2 dd, −23 m. MS (ESI): calculated for $C_{14}H_{23}N_5O_{12}P_3S_3^-$ (M^-) 641.97; found 641.9.

2′-Deoxy-2′-(*t*-butylthio)uridine-α-thiotriphosphate. ^{31}P NMR (D_2O, 400 MHz): δ 46.1 m, −8.0 dd, −22.4 m. HRMS (FAB): calculated for $C_{13}H_{22}N_2O_{13}P_3S_3^-$ (M^-) 602.9502; found 602.9526.

Transcription Reactions. ΔC209 P4−P6 was transcribed from *Ear*I digested ΔC209 plasmid (gift from K. Juneau and T. Cech). Transcription reactions contained 40 mM tris(hydroxylmethyl)aminomethane hydrochloride (Tris-HCl, pH 7.5), 4 mM spermidine, 10 mM dithiothreitol (DTT), 15 mM $MgCl_2$, 0.05% Triton X-100, 1.0 mM NTPs, 0.05 μg/μL DNA template, and 0.08 μg/μL Y639F T7 RNA polymerase. In separate reactions 2′-mercapto-α-thiotriphosphates were added at the following concentrations: 0.4 mM A_{SH}αS, 0.5 mM G_{SH}αS, 0.4 mM C_{SH}αS, and 0.4 mM U_{SH}αS. All transcription reactions were incubated for 2 h at 37 °C. The N_{SH}TPαS concentrations were chosen to achieve a level of approximately 5% analogue incorporation, determined by comparing I_2-induced cleavage intensities to a NTPαS standard.[8b,f,g] Transcripts were purified by denaturing PAGE (10 mM DTT in gel and buffer). Samples were eluted, and ethanol was precipitated, washed with 70% ethanol, and resuspended in 1X TE with 10 mM DTT.

Biotin/Streptavidin Gel Shift Assay Verifying 2′-SH Integrity. To ensure that the mercapto group remains intact following transcription and isolation of the RNA, the transcripts were treated with a mercaptan modifying reagent. Modification was detected by observing a difference in gel mobility due to the increased steric bulk introduced by the modification reagent (biotin/streptavidin). Maleimide-PEG_3-biotin contains a maleimide group linked to biotin that reacts predominantly with free −SH groups at pH 8.0. Selective alkylation of the mercapto group covalently attaches the biotin moiety to the transcript. Modification with maleimide-PEG_3-biotin alone resulted in a gel shift of short RNAs (6−12 nt; data not shown); however, due to the length of P4-P6 (∼160 nt), a gel shift was not observed. Subsequent reaction of the biotinylated species with streptavidin resulted in a gel shift, where the single band of the unmodified material became a smear with lower mobility. The smear is likely due to the variability in the number of residues containing the 2′-mercapto analogue in a single transcript (approximately 1−5 substitutions per transcript). Because the 2′-SH transcripts also contained a phosphorothioate linkage, transcriptions with 2′-OH α-thiotriphosphates (also containing a phosphorothioate linkage) were included as controls to ensure that modification was specific to the 2′-mercapto group.

Cold RNA (∼10 pmol) or radiolabeled RNA (∼20 pmol) was modified with maleimide-PEG_3-biotin (10 mM) in 50 mM HEPES pH 8.0, 300 mM NaCl, and 1 mM EDTA. The reactions were incubated at room temperature for 2 h, and extracted with phenol/chloroform/isoamyl alcohol (25:24:1) followed by extraction with chloroform. The samples were resuspended in water and treated with 20 mM HEPES pH 7.4, 1.0 M NaCl, 5 mM EDTA, and 15 μg of streptavidin. The reactions were incubated at room temperature for 20 min and quenched with an equal volume of 90% formamide, 1X TBE (89 mM Tris; 89 mM boric acid; 2 mM EDTA). Nonradioactive samples were run on 1% agarose gels and visualized by ethidium bromide staining. Radioactive samples were run on DPAGE. Modification by biotin/streptavidin resulted in a slower migrating band or smear as compared to that of the unmodified transcripts.

Nondenaturing Gel Electrophoresis. Nondenaturing gels were electrophoresed in a manner similar to that of Silverman and Cech.[13a] Gels were cast with 8% acrylamide, TB (89 mM Tris; 89 mM boric acid; pH 8.3), 2.0 or 0.45 mM $MgCl_2$, 0.05 mM EDTA, and 10 mM DTT and allowed to polymerize overnight. Electrophoresis buffer contained the same components as the gel. Gels were electrophoresed at room temperature at 150 V for 5 h. The temperature of the gel buffer was checked periodically. Fluctuation in temperature was not observed under the electrophoresis conditions.

Folding Reactions. Transcripts were treated with calf alkaline intestinal phosphatase (Amersham Pharmacia) and 5′-end-labeled with [γ-^{32}P]-ATP (Perkin-Elmer Life Sciences) and T4 polynucleotide kinase (New England Biolabs) according to the manufacturer's instructions. The samples were purified by DTT PAGE (10 mM DTT), and the integrity of the mercapto group was verified by gel shift assay. Folding reactions contained 5′-radiolabeled RNA, 2.0 or 0.45 mM $MgCl_2$, TB (pH 8.3), 10 mM DTT, and 5% glycerol. The samples were heated at 50 °C for 5 min and allowed to cool at room temperature for 10 min before loading on the native gel. The bands were visualized by autoradiography, excised, and eluted into TE (10 mM Tris·HCl pH 7.5, 1 mM EDTA) at 4 °C overnight. The samples were ethanol precipitated and resuspended in 10 μL of 50 mM HEPES (pH 8.0), containing 100 mM iodoacetamide. Iodoacetamide modification prior to sequencing reduces smearing during electrophoresis, thereby improving resolution, and prevents modification of the mercapto group during I_2-induced cleavage. The iodoacetamide reaction was allowed to proceed for 15 min. The reactions were then quenched and purified by DPAGE. The bands were visualized by autoradiography, excised, and eluted into TE at 4 °C for 4−6 h. The samples were ethanol precipitated and washed with 70% ethanol.

I_2 Sequencing. The samples were resuspended in 10 μL of gel loading solution and split into two fractions. One fraction was treated with 1/10 volume 100 mM I_2 in ethanol. The samples were heated to 90 °C for 1.5 min and loaded on a 9% DPAGE gel. The samples were electrophoresed for varying amounts of time so as to achieve the best resolution of the residues near the ends of the transcripts.

Interference Quantitation. Interference values were assigned essentially as described in Ryder et al.[8g] Peak intensities were quantitated by PhosphorImager analysis at each residue for the selected and unselected lanes. Values were normalized against total intensity for each lane to account for loading differences. Interference was calculated at each position according to the equation:

$$\text{interference} = \frac{\dfrac{\text{NαS 0.45 or 2.0 mM } Mg^{2+} \text{ selected lane}}{\text{2′-H or 2′-SH 0.45 or 2.0 mM } Mg^{2+} \text{ selected lane}}}{\dfrac{\text{NαS unselected lane}}{\text{2′-H or 2′-SH unselected lane}}}$$

The data were normalized to give a value of 1 where no interference occurs.[8g] Each interference value was determined from at least three independent experiments.

Computer Modeling. Space-filling models of the ΔC209 P4-P6 domain (PDB accession: 1HR2)[9h] were generated using Chem3D version 5.0 (CambridgeSoft Corp.). 2′-Mercapto substitution was modeled by replacing the 2′-oxygen with 2′-sulfur. The bond length

was increased to 1.819 Å, the average C−S bond length from gas-phase molecules.[27] Close contacts were calculated and tabulated for each residue using Chem3D and the modified models. Sites at which the increased steric bulk of the 2′-SH substitution could not be accommodated without overlapping of nearest neighbor van der Waals radii were designated as sites of steric clash. This designation excluded sites at which the steric clash arose from a neighboring atom within the same residue, such as the 3′-oxygen.

Acknowledgment. The authors thank Professor Rui Sousa for the gift of the Y639F T7 RNA polymerase plasmid, Kara Juneau and Professor Tom Cech for the ΔC209 P4-P6 plasmid, and Professor Michelle Hamm and members of the Piccirilli lab for comments on the manuscript. J.A.P. is an associate investigator of the Howard Hughes Medical Institute.

Supporting Information Available: Representative non-denaturing gel and enlarged space-filling space models for Figure 4 (PDF). This material is available free of charge via the Internet at http://pubs.acs.org.

JA035175Y

(27) Liede, D. R., Ed. *CRC Handbook of Chemistry and Physics*, 73rd ed.; CRC Press: Boca Raton, FL, 1992; pp **9**-15−41.